# Formation, stability, and atomic structure of the Si ( 111 ) – ( 6 x 6 ) Au surface reconstruction: A quantitative study using synchrotron radiation

R. Daudin, T. Nogaret, A. Vaysset, T. Schulli, A. Pasturel, Gilles Renaud

# Formation, stability and atomic structure of the Si(111)-(6×6)Au surface reconstruction: a quantitative study using synchrotron radiations

R. Daudin,[1,*] T. Nogaret,[2] A; Vaysset,[1,†] T.U. Schülli,[3] A. Pasturel,[2] and G. Renaud[1]

[1] *Univ. Grenoble Alpes, INAC-S2PM and CEA, INAC-SP2M, F-38000 Grenoble, France.*
[2] *Science et Ingénierie des Matériaux et des Procédés, INP Grenoble, UJF-CNRS, 1130, rue de la Piscine, BP 75, 38402 d'Héres Cedex, France*
[3] *Beamline ID01, European Synchrotron Research Facility, 6 rue Jules Horowitz, BP 220 F-38043 Grenoble CEDEX 9, France*

(Dated: December 2, 2014)

The conditions of formation of the Au-induced Si-(6×6) reconstruction, its stability as well as its atomic structure are studied experimentally using grazing incidence X-ray diffraction techniques. This reconstruction is found to form at 680 K when cooling down eutectic droplets previously obtained by the dewetting of thin gold films (of various thickness) deposited at room temperature on a Si(111) substrate. The quality of the reconstruction is found to depend on the annealing temperature. The formation of the (6×6) reconstruction at low temperature after it has been destroyed by ion bombardment, together with the recovery of the Si surface gives evidence of its high stability and highlights the surfactant properties of gold atoms.
The determination of the Si(111)-(6×6)Au atomic structure is performed using quantitative surface X-ray diffraction with an existing complex model proposed in the literature as a starting structure. The resulting gold structure is found to be 1 ML thick and consists in two domains related by a mirror. They are composed of trimer and pentagonal units with special sites presenting a partial occupancy of 0.5. Our experimental dataset does not provide enough accuracy to determine the positions of the Si atoms of the substrate but *ab-initio* calculations tend to confirm that they are only slightly displaced from the bulk position.

PACS numbers: 68.35.B-, 68.49.-h, 61.05.cf
Keywords: gold; silicon; X-ray diffraction; surface reconstruction.

## I. INTRODUCTION

Gold is a metal known to induce many surface reconstructions when it is deposited on a Si(111) substrate. For coverage ranging from 0 to 2 ML (one monolayer (ML) corresponds to a deposited thickness of 2.35 Å), (5×2), ($\sqrt{3}\times\sqrt{3}$)R30° and (6×6) reconstructions are the most common and have been intensively studied over the last two decades. Many attempts have been made to draw a correct picture of the phase diagram presenting the different reconstructions as a function of coverage and temperature. Plass *et al.*[1] proposed a submonolayer phase diagram. Their work was further developed by Grozea *et al.*[2] to extend the phase diagram up to 2 ML coverage. The complexity of this system comes from the domains of existence of the reconstructions that are difficult to define precisely as they depend over wide ranges on the amount of Au deposited as well as on the temperature. In addition, the phase transitions are still unclear due to difficulties to get the detailed atomic structures of each phase, which are still under debate. This is even more complicated considering that small Au particles can nucleate and grow at various temperatures in parallel to the different reconstructions[3,4]. The (5×2) reconstruction is known to form in the submonolayer regime in a quite wide coverage range at low temperature (400 K) from 0.1 ML up to 0.7 ML, which narrows with increasing temperature (only up to 0.5 ML at 1000 K). The ($\sqrt{3}\times\sqrt{3}$)R30° surface reconstruction can be found in a wide range of coverage and temperature. Moreover, it is necessary to distinguish between two phases: $\alpha$-($\sqrt{3}\times\sqrt{3}$)R30° (0.5-1 ML, 400-900 K) and $\beta$-($\sqrt{3}\times\sqrt{3}$)R30° (1-2 ML, 650-800 K). These two structures, which have the same periodicity, seem to differ in their chemical environment and in the density of their domain walls[5]. The (6×6) is known to form generally above 1 ML and is stable up to about 700 K. All these reconstructions were found to be stable above the Au-Si eutectic temperature ($T_e$=636 K), suggesting potential stabilization of Au-Si bonds by surface processes. Other reconstructions were also reported such as (2×2)[6], ($2\sqrt{3}\times2\sqrt{3}$) and ($2\sqrt{21}\times2\sqrt{21}$)R±10.9°[7], the latter being related to the energetically favored in-plane orientation relationship reported elsewhere[8].

The first observation of the Au-induced Si(111)-(6×6) reconstruction was reported by Lander[9]. Since then it has been studied using scanning tunneling microscopy (STM)[10–14], transmission electron diffraction (TED)[15,16], Auger electron spectroscopy[17], X-ray diffraction (XRD)[18,19], low energy electron diffraction (LEED)[4,9,11,13,17,20,21], impact-collision ion-scattering spectroscopy (ICISS)[22] and reflection high energy electron diffraction (RHEED)[7,23,24]. Dealing with the (6×6) reconstruction can not be done without mentioning the ($\sqrt{3}\times\sqrt{3}$)R30° as many studies reveal a clear link between the two structures. The LEED study of Higashiyama *et al.* [20] reports a transition from a (6×6) pattern to a ($\sqrt{3}\times\sqrt{3}$)R30° + ring like pattern by an-

nealing at high temperature, the transition being reversible. This agrees well with TED measurement[15] which revealed that the (6×6) pattern can form by increasing the coverage from the ($\sqrt{3}\times\sqrt{3}$)R30° + star pattern at low temperature or by decreasing the temperature from the ($\sqrt{3}\times\sqrt{3}$)R30° + ring/hexagon pattern at high coverage. The creation of the (6×6) reconstruction by cooling the sample from higher temperatures where the ($\sqrt{3}\times\sqrt{3}$)R30° reconstruction is present indicates a need of activation energy but at the same time, the (6×6) was also found to be unstable above 600 K, claiming for weak binding energy in this study. The cooling rate was also reported to influence the resulting surface structure[14]. STM observations performed at room temperature and reported by Nogami *et al.* [21] also revealed a continuous transition from ($\sqrt{3}\times\sqrt{3}$)R30° to (6×6) : the ($\sqrt{3}\times\sqrt{3}$)R30° domains (with domain walls running along the <121> substrate directions) decrease in size with increasing coverage to form a well ordered (6×6) structure. In this study the transition was not found to be reversible.

A complementary STM/LEED study[11] claims for the co-existence of two ($\sqrt{3}\times\sqrt{3}$)R30° domains (one ordered and one disordered) at 0.7 ML. With increasing coverage, the ordered domains disappear and LEED measurements show that disordered domains turn into (6×6) structures. At the same time, the (6×6) unit cell is not visible by STM whereas rectangular arrays of "protrusion" with smaller periodicity than the (6×6) are seen. The authors concluded that the (6×6) structure consists in a network which composes the domain walls that separate the ($\sqrt{3}\times\sqrt{3}$)R30° domains. Another combined LEED/STM study from Salvan *et al.* [17] reports the observation, at 1 ML Au coverage, of a ($\sqrt{3}\times\sqrt{3}$)R30° LEED pattern but with STM images displaying local (6×6) structures: the proposed model consists in a (6×6) structure composed of structural units of $\sqrt{3}$ periodicity. Thanks to the ICISS technique, a study[22] proposed a model of the (6×6) reconstruction consisting of a combination of simple honeycomb and centered hexagons with no position variations of the underlying Si atoms as well as no mixing between the species. The ($\sqrt{3}\times\sqrt{3}$)R30° structure, with empty hexagons presenting no long range order, is seen as a precursor of the (6×6) structure which forms by filling the hexagons with additional Au atoms. Dornisch *et al.* [18] used in-plane surface X-ray diffraction to determine the atomic structure. Their study confirmed the trimer model previously proposed by Oura *et al.* [25] for the ($\sqrt{3}\times\sqrt{3}$)R30° reconstruction. They claim that the (6×6) reconstruction is not a superstructure of the ($\sqrt{3}\times\sqrt{3}$)R30° but that the atoms deeply rearrange themselves in a structure composed of two sixfold twinned domains. The gold atoms arrange themselves in turned trimer triplets with additional Au sites in between. From the Patterson function, the Au-Au distance was found to be 2.8 Å. This trimer organization is also supported by TED and HRTEM measurements from Plass *et al.* [16] and a recent STM+LEED study in which partial disorder in the (6×6) structure was observed[13].

A more complex model has been suggested by Grozea *et al.* [19] by re-analyzing the surface X-ray diffraction data of Dornisch *et al.* using a "direct method"[26,27] to determine the surface structure. They proposed that the (6×6) atomic structure can be described as a combination of pentagonal and trimers units with a fixed Au-Au distance.

Despite intense research on this topic, this reconstruction still remains mysterious and controversial in terms of formation processes, stability and atomic structure. In this paper, Grazing Incidence X-ray Scattering (GIXS) is used *in-situ*, in UHV (Ultra High Vacuum) to study the conditions of formation of the Si(111)-(6×6)Au reconstruction (as well as the Si(111)-($\sqrt{3}\times\sqrt{3}$)R30°Au ) but in the case of thick deposited gold films (typically ∼7 ML) that dewet with annealing and form islands/droplets in coexistence with a wetting layer of the order of one monolayer thickness[8,28]. The formation of the Si(111)-(6×6)Au reconstruction is found to appear around 680 K when cooling down the sample from higher temperature, the process being reversible. The quality of the reconstruction is found to depend on the annealing temperature. Moreover, the structure of the (6×6) reconstruction has been determined by quantitative analysis of X-ray measurements and refinement methods. Finally, *ab-initio* calculations were performed to obtain additional information on the stability of the atomistic model used to investigate the Si(111)-(6×6)Au reconstruction.

## II. MATERIALS AND METHODS

### A. Sample preparation

The X-ray experiments were performed at the ESRF (European Synchrotron Radiation Facility, Grenoble, France) on the BM32 beamline[29], using a UHV chamber equipped with large beryllium windows for x-ray transparency. It has a base pressure of $10^{-10}$ mbar. This chamber, which has been designed for surfaces, interfaces and nanostructures studies under ultra high vacuum, is coupled to a surface diffractometer[30].

The heating component consists in an electron-bombardment set-up placed behind the sample holder and the temperature of the sample is measured with two IRCON infrared pyrometers. They are placed outside the chamber behind a sapphire viewport and cover a temperature range from 470 K to 2200 K with an accuracy estimated to $\pm 5$ $K$. They have been calibrated in the temperature range of the present study at the melting points of ultra pure lead (600 K) and of bulk $Al_{88}Si_{12}$ eutectic (850 K).

For each experiment, the 10×10 mm$^2$ Si(111) samples were prepared as follow:

- outgassing at 500 K during 24 hours in a preparation chamber to remove organics impurities,

- transfer into the growth chamber and de-oxidation at 1200 K under UHV conditions ($10^{-10}$ mbar),
- acquisition of a clear diffraction pattern (by *in-situ* GIXS and RHEED) corresponding to the formation of a well-defined Si(111)-(7×7) surface reconstruction, without SiC features, which are clear indications of a clean Si(111) surface[31].

The deposition of gold on the Si substrates is performed by evaporation of the metal at RT using a Knudsen cell with a flux of 0.4 Å.min$^{-1}$. The deposition rate was calibrated using a quartz microbalance and X-ray reflectivity.

### B. X-ray measurements

GIXS experiments were performed with a 11 keV incident beam at a fixed incident angle $\alpha_i$ of 0.163°, equal to the critical angle for total external reflection for silicon at this energy. This allows enhancing surface versus bulk scattering. The sample and the detector are positioned with regard to the beam direction by the angles ($\omega$,$\alpha_i$) and ($\delta$,$\alpha_f$), respectively. The measured diffracted intensity in reciprocal space ranges from 0.5 to 8.5 Å$^{-1}$ of the momentum transfer $Q$. This latter is defined as $\mathbf{Q} = \mathbf{k_f} - \mathbf{k_i}$, with $\mathbf{k_i}$ and $\mathbf{k_f}$ the wave vectors of incident and scattered beams, respectively, so that $\|\mathbf{Q}_{\|}\| = (4\pi/\lambda)\sin(\delta/2)$ where $\delta$ is the in-plane scattering angle between $\mathbf{k_i}$ and $\mathbf{k_f}$ and $\lambda$ the X-ray wavelength. To avoid any confusion, we present hereafter the different types of scans discussed in this study, each scan giving structural information in the direction of the measurement:

- *rocking-scans* are done by a rotation $\omega$ of the sample around its surface normal at a constant $Q$ (i.e with all other angles fixed),
- *radial-scans* are those performed along a given substrate azimuth (varying $\delta$ and $\omega$ with fixed $\alpha_i$ and $\alpha_f$),
- out-of-plane scans along $Q_\perp = k(sin(\alpha_i)+sin(\alpha_f))$ are performed by varying $\alpha_f$ with fixed $\alpha_i$ and are called $Q_\perp$*-scans*.

The collection of the set of data consisted in performing highly resolved *rocking-scans* on each (6×6) reflection, over a 120° segment of reciprocal space. All reflections were integrated and corrected for monitor, area, Lorentz and polarization corrections[32,33]. The substrates' Bragg reflections and crystal truncation rods (CTRs) were removed to avoid bulk contributions, the remaining set of data thus consists in 976 in-plane reconstruction structure factors.

The surface unit cell ($\mathbf{a_s}$,$\mathbf{b_s}$,$\mathbf{c_s}$) of the Si(111) substrate is conventionally defined with $\mathbf{a_s}=(1/2)\times(\mathbf{b_b} - \mathbf{a_b})$, $\mathbf{b_s}=(1/2)\times(\mathbf{c_b} - \mathbf{b_b})$ and $\mathbf{c_s}=\mathbf{a_b} + \mathbf{b_b} + \mathbf{c_b}$ with $\mathbf{a_b}$, $\mathbf{b_b}$ and $\mathbf{c_b}$ the primitive bulk lattice vectors. The Si(111)-(6×6)Au reconstruction (which is six times larger) is thus defined with the surface unit cell ($\mathbf{a_s^6}$,$\mathbf{b_s^6}$,$\mathbf{c_s^6}$)=(6×$\mathbf{a_s}$,6×$\mathbf{b_s}$,$\mathbf{c_s}$). For convenience, in this paper, the diffraction data (graphs, structure factors, etc...) are given in terms of the surface reciprocal lattice units (s.r.l.u.) $h_s$ and $k_s$ in the basis of the Si(111)-(6×6)Au reconstructed surface unit cell. With this definition, any (6×6) peak is located at integer values of $h_s$ and $k_s$.

### C. Ab-initio calculations

To study structural and energetic properties of the Si(111)-(6×6)Au reconstruction, we performed total energy calculations using the Vienna *ab-initio* simulation package[34].The Perdew-Wang exchange-correlation potential[35] and the projected augmented wave method[36] were used to describe the electronic structure of the system. The plane-wave cutoff was set to 300 eV and only the Γ point sampling was used to perform Brillouin-zone sampling. We used a supercell constituted of a 10 Å vacuum layer and a Au monolayer on top of 6 Si(111) bilayers. The dangling bonds of Si atoms of the bottom are hydrogenated. Au atoms are arranged according to the (6×6) atomic structure proposed by Grozea *et al.* [19]. The supercell contains 513 atoms and structural optimizations were carried out to ensure that all residual forces on atoms are smaller than 0.01 eV/Å.

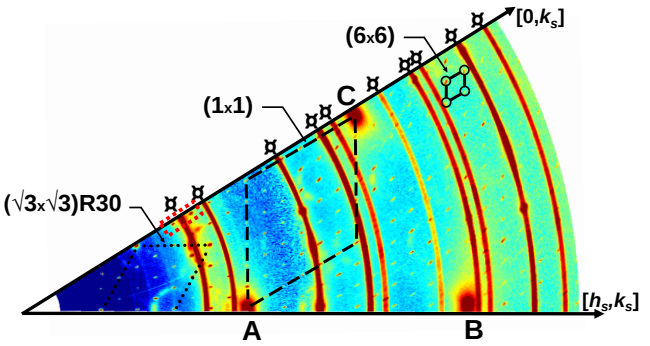


FIG. 1. Reciprocal space map covering 30° of the reciprocal space (between the [110] and [010] surface directions) recorded in the solid state at RT after a 7 ML deposit performed at RT, annealed at 700 K (liquid) and subsequently cooled down. The red colors correspond to high intensities whereas blue ones correspond to low intensities and green to intermediate. This map clearly shows the Si monocrystal Bragg peaks: A=Si($2\bar{2}0$), B=Si($4\bar{4}0$) and C=Si($2\bar{4}2$) (expressed here with bulk indexes). It also shows the Au polycrystalline Debye-Scherrer rings (symbol) as well as the mesh of thin peaks corresponding to the (6×6) reconstruction. The red-dashed line highlights the location of the *radial-scans* of Figure 2

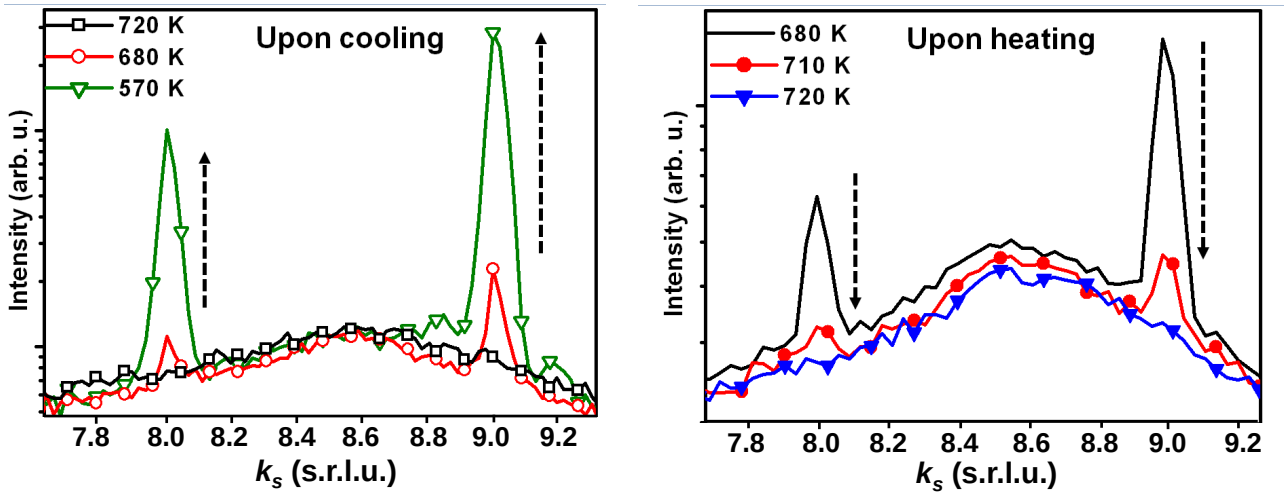


FIG. 2. *Radial-scans* performed along the [010] surface direction at the location highlighted in Figure 1, on the first maximum of the liquid signal crossing two (6×6) peaks, for a 5 ML deposit. (a) Annealed at 720 K, 680 K and 570 K. (b) Upon heating at 680 K, 710 K and 720 K. $k_s$ is given in terms of reconstructed surface reciprocal lattice unit (s.r.l.u), the two recorded (6×6) reconstruction peaks are thus located at $k_s = 8$ and 9 for the selected range.

## III. EXPERIMENTAL RESULTS

### A. Formation of the Si(111)-(6×6)Au reconstruction

A standard experiment consisted in depositing a gold film of several ML (typically 7 ML) thickness at RT followed by annealing at higher temperature. At the Au-Si eutectic temperature ($T_e$=636 K), the Si atoms diffuse into the islands that have formed during the dewetting of the film, and the system melts[8]. The system was annealed at about 700 K. After the return to RT, a reciprocal space map, plotted in Figure 1, was recorded. It was obtained by plotting together 480 in-plane *rocking-scans*, each performed at a different $Q_{\parallel}$ value. This map displays three bulk Bragg peaks together with powder diffraction rings from polycrystalline gold. In addition, a well organized network of narrow peaks is present, corresponding to a (6×6) surface periodic superstructure. The reciprocal space of the $(\sqrt{3}\times\sqrt{3})$R30° reconstruction is also shown, having peaks forming a network turned by 30°. It is important to note here that any position of a $(\sqrt{3}\times\sqrt{3})$R30° peak is also the position of a peak of the (6×6) reconstruction. Therefore when the (6×6) reconstruction is present it is impossible to know whether or not the $(\sqrt{3}\times\sqrt{3})$R30° reconstruction is also present. Indeed, below 680 K, both reconstructions may exist.

In our experiments, annealing the sample above $T_e$ was found to be a necessary step to obtain the (6×6) reconstruction, which forms upon subsequent cooling around 680 K. If the sample is not annealed high enough, only a $(\sqrt{3}\times\sqrt{3})$R30° reconstruction remains after cooling[28].

Figure 2(a) illustrates this statement: the *radial-scans* recorded on the first maximum of the liquid signal, along the [010] surface direction, reveal no (6×6) peaks at 720 K. Well-defined (6×6) peaks only appear upon cooling at 680 K. Upon further cooling, their intensity increases to reach a maximum at 570 K, in the supercooled regime[28]. If the sample is heated again, the (6×6) reconstruction vanishes around 700 K as it is illustrated in Figure 2(b). Thus, the $(\sqrt{3}\times\sqrt{3})$R30° to (6×6) transition is found to be reversible and takes place at 680 K.

The same experimental procedure was applied to a sample onto which 30 ML of gold were deposited. After annealing at 720 K and cooling down to 570 K, the scattered intensity presents a nice liquid signal together with

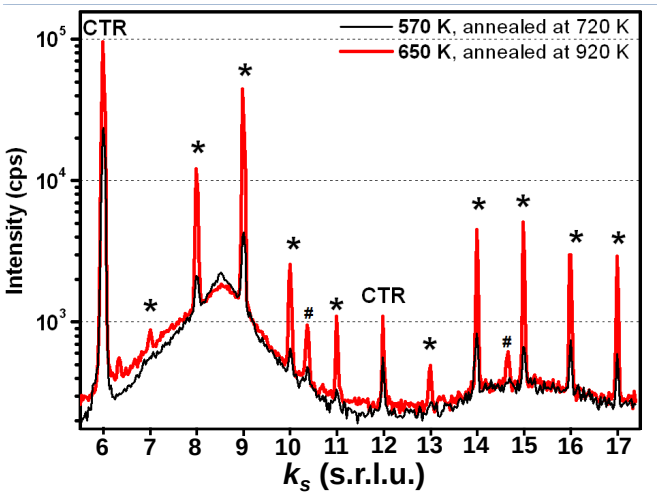


FIG. 3. *Radial-scans* along the [010] surface direction highlighting the liquid structure factor and the (6×6) signature (stars) for a 30 ML deposit of gold after annealed at different temperatures (720 K and 920 K), and cooling down below $T_e$.

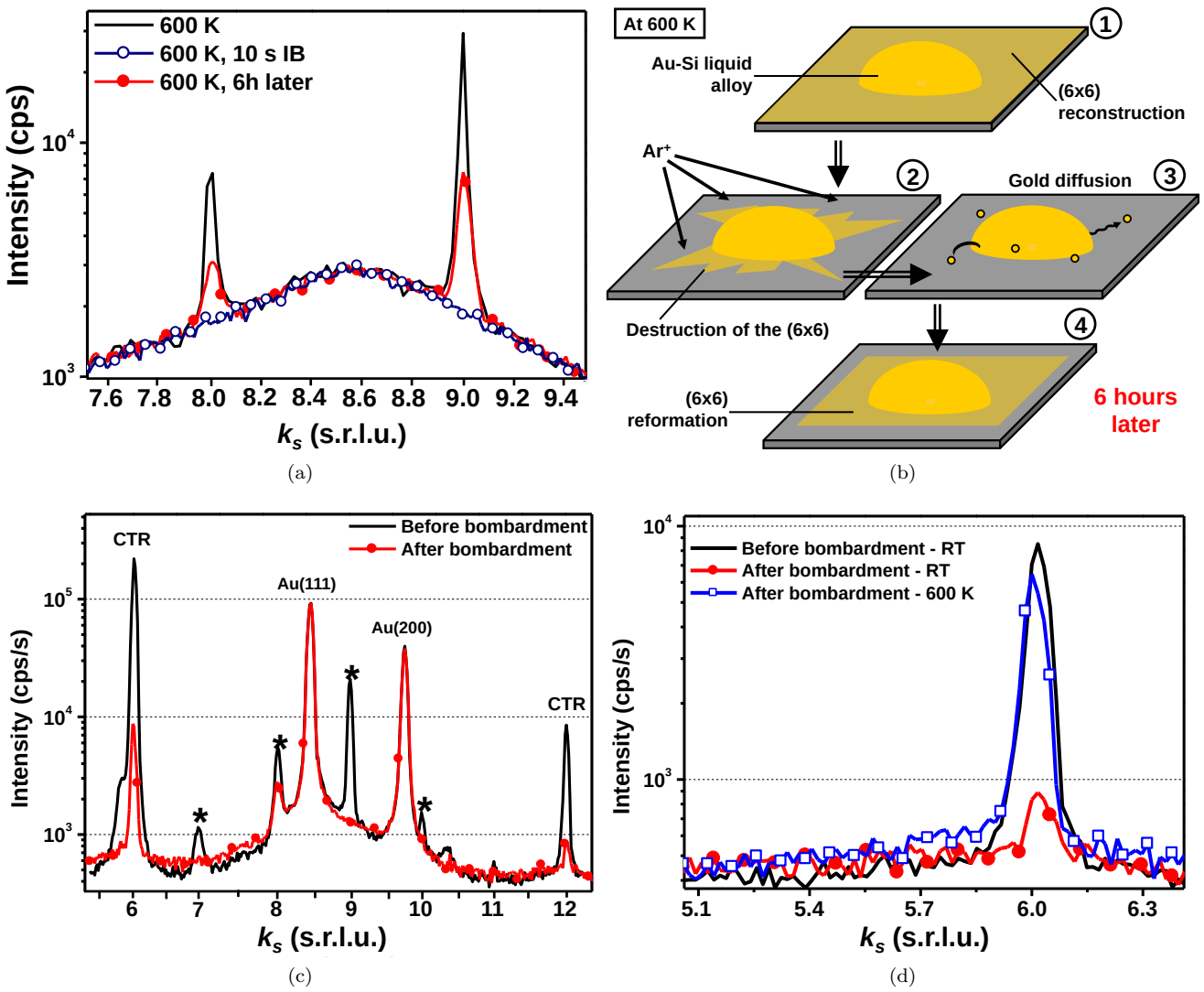


FIG. 4. (a) *Radial-scans* performed on the first maximum of the liquid signal and crossing two (6×6) reconstruction peaks (same surface direction as in Figure 2) at 600 K: before proceeding to IB, after 10 seconds of $Ar^+$ bombardment and six hours later. Between the three scans, the temperature was kept constant.(b) Scheme illustrating the reformation of the (6×6) reconstruction at 600 K. Before bombardment the droplets of AuSi alloy are surrounded by the wetting layer which is (6×6) -reconstructed, the reconstruction is then destroyed by ion bombardment, the (6×6) wetting layer re-forms by diffusion of gold atoms.(c) *Radial-scans* performed along the [010] surface direction, at RT, before and after IB. (d) *Radial-scans* on the Si substrate CTR at RT before IB, at RT after IB and annealed at 600 K.

(6×6) peaks as plotted in Figure 3. When the sample is annealed at higher temperature (i.e 920 K, below the gold evaporation temperature of 1200 K[37]), a highly enhanced (6×6) signal is measured upon cooling, even at a relatively high temperature (650 K). Unassigned peaks (#) are also recorded and are assumed to arise from 2D AuSi crystal discovered by Shpyrko *et al.* [38]. Furthermore, after high temperature annealing, the reconstruction peaks become narrower, revealing enlarged reconstruction domains. In addition, the intensities of the crystal truncation rods (CTR) in between Bragg peaks, which reflect the Si surface quality, increase when the sample is annealed at a higher temperature, suggesting that gold has a potential influence on the atomic organization of the substrate. This question will be discussed in more details in the light of additional experiments presented hereafter.

### B. Stability

During the same experiment (melting-cooling process), $Ar^+$ ion bombardment (IB) was performed on the sample in the supercooled regime (at 600 K). The (6×6) reconstruction peaks disappeared after only 10 s of bombardment (see Figure 4(a)). It implies that the long-range

ordering of the reconstruction was fully destroyed in between the droplets. The sample was then kept at a constant temperature (600 K) for around six hours. After this period the *radial-scan* shows the reappearance of the reconstruction. The peaks are smaller and wider, indicating that the reconstruction is less structured and presents smaller domains. These observations highlight different facts:

1. the system has to be annealed at least at 690 K, *i.e.* 60 K above $T_e$ to form the (6×6) upon subsequent cooling;
2. the (6×6) reconstruction is found to appear around 680 K during cooling;
3. the higher the sample is annealed, the better the reconstruction is defined (*i.e.* larger domain sizes);
4. the reconstruction can form again even at low temperature (600 K) in the presence of gold liquid droplet that seem to serve as a reservoir, as suggested in Figure 4(b).

A similar experiment has been performed with the system in the solid state. The ion bombardment was performed at RT after cooling down from 720 K. Figure 4(c) displays the *radial-scans* performed along the [010] surface direction before and after the bombardment. The comparison of the two scans reveals that the gold peaks remain the same showing that the gold islands are unaffected by the IB whereas, as for IB performed in the supercooled regime, the (6×6) peaks disappear due to the destruction of the surface structure.

The interesting feature in this case concerns the observation of the CTR evolution as their intensity (and shape) yields information on the surface roughness. Figure 4(d) shows an almost complete disappearance of the CTR with the bombardment. This means that, in addition to the destruction of the (6×6) reconstruction, the bombardment also roughens the substrate surface. If the sample is annealed again at 600 K, which is still below $T_e$, the CTR intensity is recovered (see Figure 4(d)): the substrate's smoothness improves with annealing. However, the temperature is too low to offer to the Si atoms the necessary mobility to refine the surface. As we have seen that at 600 K the Au atoms diffuse from the droplets to the substrate surface and can form again the (6×6) reconstruction, it is likely that the smoothing of the substrate surface is due to the surface diffusion of the gold atoms. These latters interact with the Si surface atoms and make their displacements possible. Indeed, it has already been reported that gold is an effective surfactant for the homoepitaxial growth of Si on Si(111) substrates. A temperature of at least 920 K is required to form Si thin films of high quality on bare surfaces[39]. However, using LEED and Rutherford backscattering spectrometry (RBS), Wilk *et al.* reported the formation of homoepitaxial Si films through an overlayer of Au at lower temperatures (720-770 K)[40]. Similar results were obtained by Minoda *et al.* by depositing the Si atoms on a Si(111)-(5×2)Au reconstructed surface[41]. The gold-covered surface was found to replace the two-dimensional growth of Si (which only occurs at the domain walls of the reconstruction) by the formation of a thin Si film between the gold reconstruction and the Si surface.

A similar experiment has been performed in this work. AuSi droplets were formed together with a (6×6) reconstruction as described above and cooled down to the supercooling regime at 600 K. The experiment consisted in recording the variation of intensity of a CTR as a function of time while Si atoms were added by MBE (see Figure 5(a)). The recorded intensity displays periodic oscillations and the elapsed time between two maxima (∼16 min) corresponds to the completion of one Si monolayer[42]. Figure 5(b) shows two *radial-scans* performed along the [110] surface direction before and after the Si deposit. The two scans are identical reflecting that the layer-by-layer growth of Si is possible even in the presence of the gold (6×6) reconstruction. This result therefore confirms that Au is an effective surfactant for Si.

A few papers have studied the AuSi droplets in parallel with the surface reconstruction. Swiech *et al.* [3] pointed out that the AuSi droplets are very mobile even at low temperature (but above 550 K). Their displacements were found to leave tracks on the substrate which prevent the formation of the (6×6) reconstruction. Conversely, the (6×6) formation was observed to start at the edges of large particles. The tracks formation has been explained later on using SEM[37]. Upon cooling, the Si present in excess in the droplet is deposited on the substrate, the particle migrates leaving a track of Si behind it with horizontal (111) orientated facets. The liquid/solid interface is therefore assumed to be very flat. Reversely, upon heating, the particles move by dissolution of the Si into the droplets.

Now that the Au-induced Si(111)-(6×6) reconstruction formation and stability conditions have been described, we focus, in the next section, on its atomic structure.

## IV. SI(111)-(6×6)AU STRUCTURE

### A. Symmetry averaging

A total of 976 in-plane reconstruction rods were measured (excluding CTRs or Bragg peaks). The in-plane diffraction pattern displayed *p6mm* symmetry, implying that the real structure could be of *p31m*,*p3m1* or *p6mm* symmetry.The measurement of equivalent reflections improves the dataset quality and allows a reduction of the systematic error by averaging the intensities of the equivalent reflections[42]. We used the AVE program[43] to average the recorded intensities in these different symmetry groups and compared the systematic errors in the dataset. For our dataset, the lowest error is obtained for the *p3m1* symmetry. The compilation of our data in this symmetry group reduces

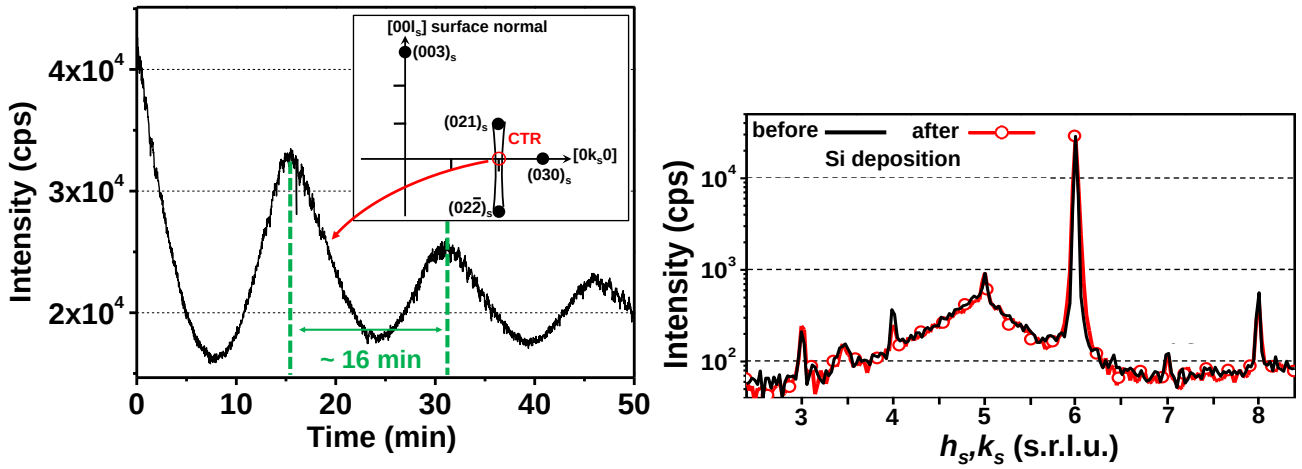


(a) (b)

FIG. 5. (a) Variation of the (200) CTR intensity as a function of time during the Si deposition. On the inset is drawn a sketch of reciprocal space of a Si(111) surface. Along the [010] in plane direction one crosses the crystal truncation rod (CTR) at the (020) position. The observed intensity at this point oscillates during Si-deposition (see text). (b) *Radial-scans* performed along the [110] surface direction before (black) and after the addition of Si in the presence of gold droplets together with a (6×6) reconstruction at 600 K.

the number of independent reflections to 441 with a mean systematic error $\epsilon$ of 3.9 %. The result is plotted in Figure 6 for the *p3m1* symmetry. All independent experimental structure factors are listed in Table I of Supplemental Material. The errors $\sigma$ calculated from statistical and systematic errors[44] are also given together with the theoretical structure factors deduced from the refined model presented in section IV B. The agreement criterion with the experimental ones is provided by the normalized chi-squared ($\chi^2$ )[43].

### B. Model Evaluation

An analysis of the width of the *rocking-scans* on (6×6) peaks yields information on the average domain size. An example is given on the inset of Figure 6 showing a *rocking-scan* performed on one of the most intense fractional-order (6×6) peak. A Lorentzian fit provides a FWHM of 0.102° (*i.e.* 0.0018 rad. at Q=2.89 Å$^{-1}$). This corresponds to an average domain size of 121 nm (exponentially decaying correlation length of 60 nm), which shows that the (6×6) reconstruction is of high quality. In addition, *l-scans* were performed on several (6×6) peaks and revealed a slow decrease in intensity perpendicular to the surface. This is typical for a rod-like shape of signals arising from surface structures, the FWHM (measured on several (6×6) rods) indicates that the thickness of this reconstruction is of the order of one monolayer.

The in-plane Patterson function calculated with our dataset (containing only fractional-order reflections of the (6×6) structure) is plotted in Figure 7. The irreducible asymmetric unit is highlighted in red. The contour plot reveals the positive peaks corresponding to interatomic vectors of the real structure[42]. According to the Patterson map, the strongest peak in the irreducible unit corresponds to a Au-Au distance of about 2.8 Å. The three arrows point out three equivalent interatomic vectors of similar length due to Au trimers which are the prominent structural elements of the Si(111)-Au($\sqrt{3}\times\sqrt{3}$)R30° and of the Si(111)-Au(6×6) structures[18]. The refined model proposed by Dornisch *et al.* was still incomplete and our Patterson map displays additional peaks corresponding to representative interatomic distances that have to be considered in the model. Despite the apparent simplicity of the Patterson map and many efforts to propose a trial structure based on Au trimers completed with either Au or Si atoms to fit the other interatomic distances, no satisfactory model could be deduced. By applying a direct method to the SXRD data of Dornisch *et al.*, Grozea *et al.* [19] have been able to propose a model of the atomic structure of the Au-(6×6) reconstruction represented in Figure 8. The proposed surface structure consists in a hexagonal structure with an almost *p3m1* symmetry. In Figure 8, the gray atoms are the 14 independent sites, the equivalent atoms related by *p3* symmetry have the same number. In green are highlighted the sites on the 3-fold symmetry axes having a partial occupancy (see later). In addition, Grozea *et al.* mention the presence of twin domains. More interestingly this structure is composed of two kinds of motifs: the motif A which is partially occupied, and the motif B which presents two rotational variants. A combination of pure empty A and B motifs corresponds to a structure with a $\sqrt{3}$ periodicity.

The model displays sub-structural units composed of

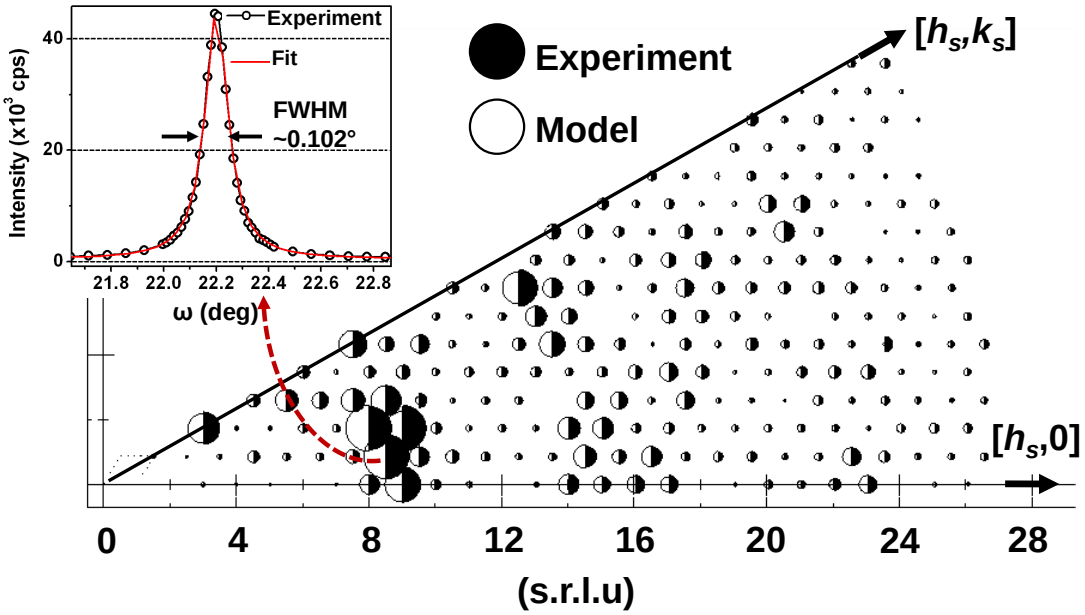


FIG. 6. Experimental structure factors using *p3m1* symmetry (in black), together with the final model structure factors (in white). The area of the circles is proportional to the reflection's intensity. The experimental and model circles are of same sizes (*i.e.* same intensity) for all reflections illustrating the final agreement $\chi^2$ of 1.3. Inset: *rocking-scan* performed on the (8,6,0) reconstruction peak.

gold trimers, in agreement with the structure proposed by Dornisch *et al.* , but also incomplete and complete pentagons (Figure 8) that would explain the difficulties to find a proper model with classical methods. In addition to gold atoms, Grozea *et al.* proposed significant displacements of the Si atomic structure in the first layers which were found necessary to improve the agreement between the model and their experiment. They also revealed the existence of a strain field in the substrate which strongly displaces the Si atoms in the first layers.

In the present work, we use the model of Grozea *et al.* as a trial model for a standard structure refinement and propose to dispel several uncertainties of their study. Our experimental structure factor dataset contains much more reflections than their dataset (about four times more). The systematic uncertainty of their measurements ($\sim$10 %[18]) is much higher than the present one and despite that, their $\chi^2$ value remains rather high[45]. The reduction of their $\chi^2$ has been obtained only through strong assumptions and their experimental measurements imposed a transfer of the sample into a baby chamber, which could have influenced the results.

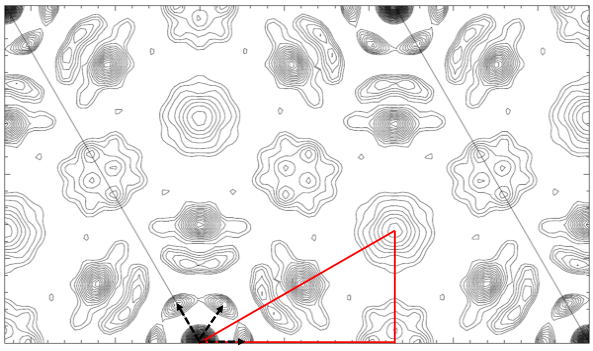

FIG. 7. Experimental fractional-order Patterson function plotted in the (6×6) unit cell. The three arrowed peaks are known to be due to trimers of Au.

In the following, we present our structure refinement of the (6×6) reconstruction by confronting Grozea's model to our own set of X-ray data. More interestingly, our data were collected under completely different experimental conditions (sample preparation, UHV chamber, film thickness, annealing, *in situ* measurements etc.), it is thus even more important to compare the two (6×6) structures.

The first $\chi^2$ minimization was performed with only the Au atoms taken into account. The model used consisted in the hexagonal structure presented in Figure 8 with 45 gold atoms. All atoms were assumed to have the same Debye-Waller (DW) factor as well as the same occupancy. Their displacements were allowed with respect to the *p3m1* symmetry, which means that the special atoms were assumed to be immobile and that the different sets of three related atoms were constrained in directions respecting the imposed symmetry. The evaluation of this model gives a $\chi^2$ value of 10.1, which is a good value regarding the simplifications imposed. This agreement confirms that the structure proposed by Grozea *et al.*, which is quite surprising at first sight, is a very good model candidate. The twin domains, mentioned by Grozea *et al.*, which are assumed to scatter incoherently (*i.e.* to be far

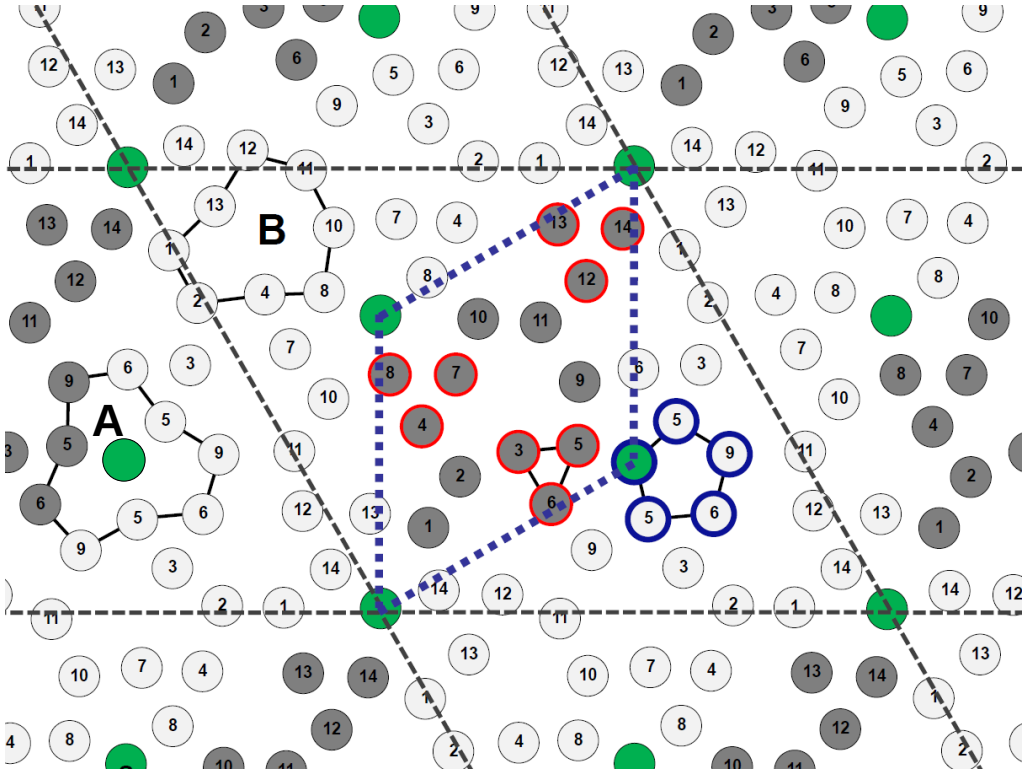


FIG. 8. Scheme of the Au-(6×6) hexagonal lattice (dashed-black line). It is composed of 45 atoms: 14 independent sites (grey atoms in dashed-blue hexagonal primitive lattice) from which the 28 others can be deduced by the *p3* symmetry (the equivalent atoms have the same number). The 3 other atoms (green) are special sites on p3 axes, and are partially occupied (see text). The structure is also completely described by tiling the plane with the highlighted A and B motifs that are formed by sub-structural trimers (red) and pentagons (blue).

from each other) are deduced by a mirror placed along the long diagonal of the (6×6) unit cell. The addition of an incoherently scattering second domain in the fit procedure reduced the $\chi^2$ to 5.8. This result can be improved further by focusing on the special sites. Grozea *et al.* pointed out that the gold atoms located on the symmetry axis display a partial occupancy of 0.504±0.004. To take into account this potential difference, distinct occupancy as well as DW parameters were attributed to the special atoms. This led to a decrease of the $\chi^2$ value down to 3.1, and the occupancy value of the special atoms dropped to 0.49±0.015, whereas the occupancies of other atoms remained equal to 1.

These results demonstrate that with only gold atoms, the model proposed by Grozea *et al.* is already in very good agreement with our SXRD data. The $\chi^2$ value is even much smaller with the present dataset, despite the much lower uncertainties. However, to improve their $\chi^2$ value, Grozea *et al.* had to include several Si bilayers subjected to a strain field that displaces the atoms far from their bulk positions, especially in the first layer.

Here, by simply adding a Si(111) bilayer below the gold reconstruction, at the bulk position, with an occupancy assumed to be equal to 1, the $\chi^2$ value decreased to 1.85 with the Si atoms only slightly displaced from their original positions. This result does not support Grozea *et al.* 's model as the Si atoms are not strongly displaced from their bulk ones. However the reduction of the $\chi^2$ value shows that the Si atoms contribute to the diffracted signal, even if their contribution remains weak. Finally, for a fit performed with a Si double layer with the positions given by Grozea *et al.*, with the occupancies of the Au, special Au and Si atoms assumed to be 1, 0.5 and 1 respectively, the final $\chi^2$ value is 1.3, with still very slight displacements with respect to Grozea's positions observed during the fitting. The small difference between the two $\chi^2$ values (1.85 and 1.3) does not allow to choose this last model. This model seems to be less physical because of the large displacements of the Si atoms with respect to their bulk values. Despite the fact that the Au atoms seem to have an influence on the position of the Si atoms in the first layer of the substrate, our experimental data make us believe that the most likely solution is the one for which the Si bulk positions are almost conserved. The atomic positions obtained in the last two fits can be found in Table II and III of Supplemental Material. The final in-plane DW value of non-special surface gold atoms was found to be 1.3±0.04 Å$^2$ which is twice its bulk value of 0.6 Å$^2$ (Sears[46]). Remarkably, the two-fold increase of the bulk DW term for surface atoms has already been observed during the analysis of the Au-($\sqrt{3}\times\sqrt{3}$)R30° reconstruction[16]. It was attributed to the lack of neigh-

bors providing additional degrees of freedom to the atoms to vibrate. However, the DW term for special Au atoms and Si atoms could not be refined, presenting very low ($\sim 0$ Å$^2$)[47] and very high ($\sim 2$ Å$^2$) values, respectively.

Through this model evaluation we have thus shown that the structure proposed in the paper of Grozea *et al.* agrees very well with our measurement (see Figure 6). It is particularly interesting to note that partial occupancies of special atoms as well as twin domains are fully confirmed by our analysis. Moreover, it means that this particular structure also forms in our experimental conditions which consist in a thick deposit at RT, annealed and then cooled down. Two specific features have however to be discussed here in more details: the positions of Si atoms and the partial occupancy. To investigate this and to have a deeper insight on the structural and energetic properties of the atomistic model used to interpret the Si(111)-(6×6)Au reconstruction, we performed *ab-initio* calculations at T= 0 K.

The first step consisted in studying the structural stability of the Au monolayer of the model composed of 45 atoms as shown in Figure 8. To examine the role of the substrate atoms, we explored two different configurations, the Au trimer atoms being positioned i) on top of the first Si(111) bulk layer or ii) on top of the forth Si(111) bulk layer (corresponding to our experimental view). For both configurations, we found that Au atoms barely moved from their initial positions and obtained the same conclusion for Si atoms, in close correspondence with our experiments and in disagreement with Grozea *et al.*. Calculated formation energies referred to bulk Au and Si are very close, namely 0.39 J.m$^2$ for the first configuration and 0.40 J.m$^2$ for the second one. The most striking feature is that these values are two times lower than the formation energy of an unreconstructed surface, obtained with Au atoms in epitaxial relationship with Si atoms of the first bilayer. The (6×6) reconstruction is also much more stable than configurations obtained for larger deposits at RT (>2 ML)[8].

The second step consisted in studying the partial occupancy of the (6×6) reconstruction by computing at T= 0 K the vacancy formation energies of Au atoms located at the center of the A motif (green atoms in Figure 8). For both configurations, we obtained close values around 0.1 eV. Let us mention that the formation energy of Au-vacancy for the unreconstructed surface is three times higher. Values obtained for the A motif indicate that the formation energy of this defect is small and then support their formations at higher temperatures. However the partial occupancy of $\sim 0.5$ needs to be related to a physical meaning and indicates that a Au atom can be present or not at this special position in equal proportion. This value is not attributed to the presence of a vacancy in one out of the two special sites in the structure as a fit performed with this constrain results in an increase of the $\chi^2$ value. It rather indicates the coexistence, in equiproportion, of (6×6) cells with the special sites fully occupied, and (6×6) cells with special sites unoccupied.

It is worthwhile to mention that the Si(111)-(6×6)Au reconstruction, combining gold trimers and pentagon units, has been observed by STM during the study of the location of Pb absorption site on this structure[48]. This study confirms all the main features described in the model presented above with a slight difference concerning the special sites at the corner of the unit cell, which are supposed to be absent of the structure. This is however surprising as the $\chi^2$ increases by a factor three if their occupancy is fixed at 0 in our model evaluation.

Nevertheless we found that this new configuration is still energetically favorable with respect to the unreconstructed surface since its computed formation energy is 0.43 J.m$^{-2}$. Note that all our calculations indicate that the (6×6) reconstruction tolerates some Au missing atoms in the reconstruction as observed in experiments.

## V. CONCLUSION

This paper gives a complete overview of the mechanisms controlling the formation of the Si(111)-(6×6)Au reconstruction in the case of thick Au deposits on Si(111) substrates under UHV:

-the (6×6) reconstruction is found to form only after the sample has been heated above 720 K, and cooled down below 680 K. The process is reversible: if the sample is heated again, the (6×6) disappears around 700 K,

-the higher the sample is annealed, the better the reconstruction is defined,

-the (6×6) reconstruction is very stable as it forms again after total destruction by IB, even at low temperature (600 K),

-Au is a very good surfactant for the Si(111) surface: the recovery of the Si surface by annealing only to 600 K shows that the wetting layer of gold improves the mobility of the Si atoms.

In addition we have investigated the structure of the (6×6) reconstruction from an atomistic point of view. We propose a refined model based on Grozea's one keeping in mind that they had a higher uncertainty on their data, completely different experimental conditions and made strong (but true) assumptions to minimize the $\chi^2$ value. The resulting gold structure consists in two domains, composed of trimer and pentagonal units, related by a mirror. Some special sites present a partial occupancy of 0.5 implying that they are present in one domain but not in the other.

Finally, the *ab-initio* calculations allow us to discriminate between two models having the same probability and to access the surface energies. Unlike Grozea's results, the calculations tend to confirm that the Si atoms remain very close to their bulk positions. The total calculated surface energy of the Si(111)-(6×6)Au reconstruction is found to be very small and thus confirms the great stability of this surprising surface structure.

## ACKNOWLEDGMENTS

We deeply acknowledge the ESRF for providing beamtime and the BM32 beamline staff, especially Olivier Geaymond and Olivier Ulrich for their help in setting up the beamline and experiment.


---


* Corresponding author: remi.daudin@simap.grenoble-inp.fr; Present address: Science et Ingénierie des Matériaux et des Procédés, Groupe Génie Physique et Mécanique des Matériaux BP 75 - 1130 rue de la Piscine 38402 Saint-Martin d'Héres, France

† Present address: Departement elektrotechniek (ESAT), KU Leuven, Oude Markt 13, 3000 Leuven, Belgium



[1] R. Plass and L. D. Marks, Surf. Sci. **380**, 497 (1997).

[2] D. Grozea, E. Bengu, and L. D. Marks, Surf. Sci. **461**, 23 (2000).

[3] W. Swiech, E. Bauer, and M. Mundschau, Surf. Sci. **253**, 283 (1991).

[4] Y. Nakajima, C. Voges, T. Nagao, S. Hasegawa, G. Klos, and H. Pfnür, Phys. Rev. B **55**, 8129 (1997).

[5] T. Okuda, H. Daimon, H. Shigeoka, S. Suga, T. Kinoshita, and A. Kakizaki, J. Electron. Spectrosc. **80**, 229 (1996).

[6] C. Seifert, R. Hild, M. Horn-von Hoegen, R. A. Zhachuk, and B. Z. Olshanetsky, Surf. Sci. **488**, 233 (2001).

[7] H. Sakai, E. A. Khramtsova, and A. Ichimiya, Jpn. J. Appl. Phys. **37**, L755 (1998).

[8] R. Daudin, T. Nogaret, T. U. Schülli, N. Jakse, A. Pasturel, and G. Renaud, Phys. Rev. B **86**, 094103 (2012).

[9] J. Lander, Surf. Sci. **1**, 125 (1964).

[10] A. Shibata, Y. Kimura, and K. Takayanagi, Surf. Sci. **273**, L430 (1992).

[11] T. Takami, D. Fukushi, T. Nakayama, M. Uda, and M. Aono, Jpn. J. Appl. Phys. **33**, 3688 (1994).

[12] K. Higashiyama, S. Kono, and T. Sagawa, Jpn. J. Appl. Phys. **25**, L117 (1986).

[13] K. Higashiyama, A. Egami, S. Hosoi, and K. Suzuki, Jpn. J. Appl. Phys. **40**, 6985 (2001).

[14] T. Nagao, S. Hasegawa, K. Tsuchie, S. Ino, C. Voges, G. Klos, H. Pfnr, and M. Henzler, Phys. Rev. B **57**, 10100 (1998).

[15] S. Takahashi, Y. Tanishiro, and K. Takayanagi, Surf. Sci. **242**, 73 (1991).

[16] R. Plass and L. D. Marks, Surf. Sci. **342**, 233 (1995).

[17] F. Salvan, H. Fuchs, A. Baratoff, and G. Binnig, Surf. Sci. **162**, 634 (1985).

[18] D. Dornisch, W. Moritz, H. Schulz, R. Feidenhans'l, M. Nielsen, F. Grey, and R. L. Johnson, Phys. Rev. B **44**, 11221 (1991).

[19] D. Grozea, E. Landree, L. Marks, R. Feidenhans'l, M. Nielsen, and R. Johnson, Surf. Sci. **418**, 32 (1998).

[20] K. Higashiyama, S. Kono, and T. Sagawa, Surf. Sci. **175**, L794 (1986).

[21] J. Nogami, A. A. Baski, and C. F. Quate, Phys. Rev. Lett. **65**, 1611 (1990).

[22] J. H. Huang and R. S. Williams, Phys. Rev. B **38**, 4022 (1988).

[23] E. A. Khramtsova and A. Ichimiya, Phys. Rev. B **57**, 10049 (1998).

[24] E. Khramtsova, H. Sakai, K. Hayashi, and A. A. Ichimiya, Surf. Sci. **433-435**, 405 (1999).

[25] K. Oura, M. Katayama, F. Shoji, and T. Hanawa, Phys. Rev. Lett. **55**, 1486 (1985).

[26] C. J. Gilmore, L. D. Marks, D. Grozea, C. Collazo, E. Landree, and R. D. Twesten, Surf. Sci. **381**, 77 (1997).

[27] L. D. Marks, E. Bengu, C. Collazo-Davila, D. Grozea, E. Landree, C. Leslie, and W. Sinkler, Surf. Rev. Lett. **5**, 1087 (1998).

[28] T. U. Schülli, R. Daudin, G. Renaud, A. Vaysset, O. Geaymond, and A. Pasturel, Nature **464**, 1174 (2010).

[29] `http://www.esrf.fr/UsersAndScience/Experiments/CRG/BM32`.

[30] R. Baudoing-Savois, M. D. Santis, M. Saint-Lager, P. Dolle, O. Geaymond, P. Taunier, P. Jeantet, J. Roux, G. Renaud, A. Barbier, O. Robach, O. Ulrich, A. Mougin, and G. Brard, Nucl. Instrum. Meth. B **149**, 213 (1999).

[31] P. Mark, J. D. Levine, and S. H. McFarlane, Phys. Rev. Lett. **38**, 1408 (1977).

[32] E. Vlieg, J. Appl. Crystallogr. **30**, 532 (1997).

[33] O. Robach, Y. Garreau, K. Ad, and M. B. Vron-Jolliot, J. Appl. Crystallogr. **33**, 1006 (2000).

[34] G. Kresse and J. Furthmullers, Comp. Mat. Sci. **6**, 15 (1996).

[35] Y. Wang and J. Perdew, Phys. Rev. B **44**, 13298 (1991).

[36] G. Kresse and D. Joubert, Phys. Rev. B **59**, 1758 (1999).

[37] B. Ressel, K. C. Prince, S. Heun, and Y. Homma, J. Appl. Phys. **93**, 3886 (2003).

[38] O. Shpyrko, R. Streitel, V. Balagurusamy, A. Grigoriev, M. Deutsch, B. Ocko, M. Meron, B. Lin, and P. Pershan, Science **313**, 77 (2006).

[39] F. Allen and E. Kasper, *Silicon-Molecular Beam Epitaxy*, chemical rubber, boca raton, FL ed., Vol. 1 (E. Kasper and J. Bean, 1988).

[40] G. D. Wilk, R. E. Martinez, J. F. Chervinsky, F. Spaepen, and J. A. Golovchenko, Appl. Phys. Lett. **65** (1994).

[41] H. Minoda, Y. Tanishiro, N. Yamamoto, and K. Yagi, Appl. Surf. Sci. **60-61**, 107 (1992).

[42] R. Feidenhans'l, Surf. Sci. Rep. **10** (1989).

[43] E. Vlieg, J. Appl. Crystallogr. **33**, 401 (2000).

[44] $\sigma = \sqrt{\epsilon^2 F_{hkl}^2 + \sigma_{stat.}^2}$, with $\sigma_{stat.}$ the statistical error of the considered reflection.

[45] The $\chi^2$ value is inversely proportional to the uncertainty value so that a high uncertainty lowers the $\chi^2$ .

[46] V. Sears and S. Shelley, Acta Crystallogr. A **47**, 441 (1991).

[47] This very low value might be implied by the 3-fold symmetry axis onto which these atoms sit.

[48] M. Jalochowski, Prog. Surf. Sci. **74** (2003).